Photoresponsive Formation of Gold Particles in Silica/Titania Sol−Gel Films

H. Yanagi*

Faculty of Engineering, Kobe University, Rokkodai, Nada-ku, Kobe 657, Japan

S. Mashiko

Kansai Advanced Research Center, Communications Research Laboratory, 588-2 Iwaoka, Nishi-ku, Kobe 651-24, Japan

L. A. Nagahara†

Joint Research Center for Atom Technology-Angstrom Technology Partnership, 1-1-4 Higashi, Tsukuba, Ibaraki 305, Japan

H. Tokumoto‡

Joint Research Center for Atom Technology-National Institute for Advanced Interdisciplinary Research, 1-1-4 Higashi, Tsukuba, Ibaraki 305, Japan

Received October 15, 1997. Revised Manuscript Received January 22, 1998

Fine gold (Au) particles were formed by photochemical and thermal processes in silica/titania glassy films. Photoreduction and/or thermal gelation of films dip-coated from silica/titania precursor solutions including Au(III) ions yielded gold particles. Particle formation was accompanied by changes in the surface plasmon band. The size and morphology of the particles were affected by the titania content of the mixture matrix films as well as by the gelation temperature. With higher titania contents and at higher temperatures the particle formation was accelerated and accompanied by a red shift of the absorption band. This particle formation occurred by diffusion and reduction of the doped Au(III) ions, both of which were promoted at higher titania contents. The controllable photodeposition process enabled us to form micropatterns of Au particles by using photomasks.

Introduction

Glass doped with colloidal particles has traditionally been used as stained glass, and glasses doped with metal and semiconductor particles have recently attracted much interest because their nonlinear optical behavior implies applications as photonic materials.[1−5] Moreover, single-electron tunneling phenomena in metal clusters of nanometer scale have been opening a new basis for future digital devices.[6−8] The realization of these prospective applications will require particles to be uniformly embedded and separated from each other in a suitable medium, and a variety of techniques for preparing fine particles in dielectric matrixes has been studied: photosensitive glasses,[9] ion implantation,[10] rf-sputtering,[11] plasma deposition,[12] relaxative autodispersion,[13] etc. The sol−gel process[14−16] is one promising method for incorporating a variety of functional materials in glass films, and the sol−gel coating films range over various applications such as chemical and mechanical protection,[17] optics,[18,19] electromagnetism[20,21] and catalysis.[22] For preparation of particle-doped glasses

* To whom correspondence should be addressed.
† Present address: Motorola Inc., Phoenix Corporate Research Laboratories, 2100 East Elliot Road, Tempe, AZ 85284.
‡ Permanent address: Electrotechnical Laboratory, 1-1-4 Umezono, Tsukuba, Ibaraki 305, Japan.

(1) Jain, R. K.; Lind, R. C. *J. Opt. Soc. Am.* **1983**, *73*, 647.
(2) Hache, F.; Ricard, D.; Flytzanis, C. *J. Opt. Soc. Am. B.* **1986**, *3*, 1647.
(3) Yumoto, J.; Fukushima, S.; Kubodera, K. *Opt. Lett.* **1987**, *12*, 832.
(4) Haus, J. W.; Kalyaniwalla, N.; Inguva, R.; Bloemer, M.; Bowden, C. M. *J. Opt. Soc. Am. B.* **1989**, *6*, 797.
(5) Fukumi, K.; Chayahara, A.; Kadono, K.; Sakaguchi, T.; Horino, Y.; Miya, M.; Fujii, K.; Hayakawa, J.; Satou, A. *J. Appl. Phys.* **1994**, *75*, 3075.
(6) Grabert, H., Devoret, M. H., Eds. *Single-Charge Tunneling;* Plenum: New York, 1992.
(7) Amman, M.; Wilkins, R.; Ben-Jacob, E.; Maker, P. D.; Jaklevic, R. C. *Phys. Rev.* **1991**, *43*, 1146.
(8) Andres, R. P.; Bein, T.; Dorogi, M.; Feng, S.; Henderson, J. I.; Kubiak, C. P.; Mahoney, W.; Osifchin, R. G.; Reifenberger, R. *Science* **1996**, *272*, 1323.
(9) Kreibig, U. *J. Phys. France* **1977**, *C2*, 97.
(10) Perez, A.; Treilleux, M.; Capra, T.; Griscom, D. L. *J. Mater. Res.* **1987**, *2*, 910.
(11) Nasu, H.; Tsunetomo, K.; Tokumitsu, Y.; Osaka, Y. *Jpn. J. Appl. Phys.* **1989**, *28*, L862.
(12) Kay, E. *Z. Phys. D.* **1986**, *3*, 251.
(13) Noguchi, T.; Hayashi, S.; Kawahara, M.; Gotoh, K.; Yamaguchi, Y.; Deki, S. *Appl. Phys. Lett.* **1993**, *62*, 1769.
(14) Dislich, H. *Angew. Chem., Int. Ed. Engl.* **1996**, *6*, 1879.
(15) Mazdiyasni, K. S.; Dolloff, R. T.; Smith, J. S. *J. Am. Ceram. Soc.* **1969**, *52*, 523.
(16) Sakka, S. *Treatise on Materials Science and Technology*, *22*, *Glass III*; Tomozawa, M., Doremus, R., Eds.; Academic Press: New York, 1982; p 129.
(17) Schlichting, J.; Neumann, S. *J. Norz-Cryst. Solids* **1992**, *48*, 185.

S0897-4756(97)00680-7 CCC: $15.00
Published on Web 04/21/1998

the conventional melting process has disadvantages such as limited concentration and undesirable composition of produced particles. Due to the low-temperature process involving hydrolysis and condensation reactions of metal alkoxides, the sol−gel technique was successfully applied to dope CdS microcrystals of quantum size in silica (SiO_2) glasses.[23]

The synthesis of colloidal gold (Au) particles has been widely studied by a variety of chemical methods.[24−29] The sol−gel processes have also been applied to produce Au particles in glasses. Matsuoka et al.[30] reported Au particles dispersed in SiO_2 films prepared by dip coating of an acid-catalyzed tetraethyl orthosilicate solution containing sodium chloroaurate and heating at 300−400 °C. Kozuka et al.[31] reported effects of the amount of water and/or hydrochloric acid used for hydrolysis of the silicate solution containing chloroauric acid on the size and state of the Au particles and controlled their sizes smaller than 34 nm in the SiO_2 films by heat treatment at 500 °C. Another interesting approach to forming Au particles is by using the photosensitivity of the Au complex ions.[32,33] A photoresponsive system that can be used for the light-initiated formation of Au particles in silicate gel glass monoliths has been reported by Akbarian et al.[34,35] This photogeneration is proceeded by photoreduction of gold complex ions within the gels under irradiation with ultraviolet (UV) light. They controlled the particle size by the irradiation time and pointed out the advantages of the avoidance of heat treatment and the abilty of patterning by their photoresponsive method.

In the present study we performed a photoinduced formation of Au particles in coating films by the sol−gel method using silica/titania (SiO_2/TiO_2) mixture gels. Our process is initiated by photochemical and/or thermal reduction of $AuCl_4^-$ ions, and the particle formation is controllable by the ratio of SiO_2/TiO_2. Surface plasmon absorption spectra and transmission electron microscopy (TEM) demonstrate that the photoresponsibility and thermal reactivity for the particle growth are accelerated by adding the TiO_2 component to the matrix film. This photoresponsive formation enables us to form micropatterns of Au particles in the films using photomasks. The photochemical/thermal generation process in the photopatterned Au particles is investigated by means of optical microscopy and near-field scanning optical microscopy (NSOM).

Experimental Section

Film Preparation. Thin films of SiO_2/TiO_2 containing Au(III) complex ions ($Au-SiO_2/TiO_2$) were prepared by the sol−gel process with an ethanol solution of chloroauric acid ($HAuCl_4 \cdot 4H_2O$) and a tetraethyl orthosilicate ($Si(OC_2H_5)_4$)/tetraethyl orthotitanate ($Ti(OC_2H_5)_4$) mixture under an acid catalysis. 0.01 mol of $Si(OC_2H_5)_4/Ti(OC_2H_5)_4$ mixture was added to 6 mL of a 0.05 M $HAuCl_4$ ethanol solution, and then 0.2 mL of 2 N HCl was dropped into the mixture while stirring. The ratio of SiO_2:TiO_2 (i.e., Si:Ti) in the starting alkoxide mixture was changed from 1:0 to 1:1. Deposition of films was performed by dip coating in a desiccator. The substrates used were cleaned microscope glass and fused silica slides cut to 25×10 mm^2. The substrate was uniformly coated with the sol solution by pulling it out from the solution at 5 mm/s. The coated $Au-SiO_2/TiO_2$ was dried at 150 °C for 1 min using a tube heater inside the desiccator. The film thickness was measured by a stylus profiler (Tencor, Alpha-Step 500). Gelation processes of the SiO_2/TiO_2 matrix films were examined by infrared (IR) spectroscopy using a Shimadzu FTIR-8100. The film coated on the glass substrate was mechanically scratched off and pressed into a KBr tablet for transmission measurements.

Particle Formation. The Au particles in the $Au-SiO_2/TiO_2$ films were formed by photochemical and thermal reactions. The photochemical process was performed by illuminating the sample surface at $\lambda = 365$ nm using a 250 W superhigh-pressure Hg lamp (USHIO ML-251B/A) and a filter which cut a visible portion of light. The irradiation was carried out using a bundle fiber, which was placed 5 cm above the sample surface, for 80 min at room temperature. Micropatterning by photogeneration of Au particles was done by UV irradiation through a photomask of an Al film patterned on a cover glass or a copper sheet mesh while the temperature of the specimen was kept constant between 5 and 50 °C on a Peltier block. Thermal formation of Au particles was carried out by heating the samples at temperatures between 150 and 450 °C for up to 80 min in an air oven. Formation of Au particles was examined by following the evolution of the surface plasmon resonance band using a UV−vis spectrometer (Shimadzu UV-2200).

Microscopic Observations. The morphology and size of the generated Au particles were observed by TEM. After the particles were generated by UV irradiation or heat treatment, the film was mechanically scratched off the substrate, mixed with powdered potassium chloride, and gently ground. The mixture powder was placed on top of a water surface, where potassium chloride dissolved away. Floating specimen flakes were then transferred onto a carbon-coated copper sheet mesh. TEM observations were carried out at 200 kV acceleration using a JEOL JEM-2010 electron microscope. Films micropatterned by photogenerated Au particles were investigated using an optical microscope (Olympus BX60) and NSOM. NSOM observation was performed using a commercially available system (Aurora, Topometrix, Inc.) according to the experimental setup described earlier.[36] A topographic image was recorded by maintaining a constant fiber-probe/sample distance using an optical shear-force feedback mechanism with a 3−5 mW ($\lambda_{max} = 670$ nm) diode laser. An Ar ion laser light ($\lambda = 488$ nm) beam was used with the fiber-probe to record an optical image. The light transmitted through the sample was collected by a 20×

(18) Geott-Bianchini, F.; Guglielmi, M.; Polato, P.; Soraru, G. D. *J. Non-Cryst. Solids* **1994**, *63*, 251.
(19) Arfsten, N. J. *J. Non-Cryst. Solids* **1984**, *63*, 243.
(20) Wu, E.; Chen, K. C.; Mackenzie, J. D. *Mat. Res. Soc. Symp. Proc.* **1984**, *32*, 169.
(21) Kumagai, T.; Yokota, H.; Kawaguchi, K.; Kondo, W.; Mizuta, S. *Chem. Lett.* **1987**, *1987*, 1645.
(22) Ueno, A.; Suzuki, H.; Kotera, Y. *J. Chem. Soc., Faraday Trans. 1* **1984**, *79*, 127.
(23) Nogami, M.; Nagasaka, K.; Kato, E. *J. Am. Ceram. Soc.* **1990**, *73*, 2097.
(24) Henglein, A. *J. Phys. Chem.* **1993**, *97*, 5457.
(25) Torigoe, K.; Esumi, K. *Langmuir* **1992**, *8*, 59.
(26) Yonezawa, Y.; Sato, T.; Ohno, M.; Hada, H. *J. Chem. Soc., Faraday Trans. 1* **1987**, *83*, 1559.
(27) Westerhausen, J.; Henglein, A.; Lilie, J. *Ber. Bunsen-Ges. Phys. Chem.* **1981**, *85*, 182.
(28) Quinn, M.; Mills, G. *J. Phys. Chem.* **1994**, *98*, 9840.
(29) Deki, S.; Aoi, Y.; Yanagimoto, Y.; Ishii, K.; Akamatsu, K.; Mizuhata, M.; Kajinami, A. *J. Mater. Chem.* **1996**, *12*, 4618.
(30) Matsuoka, J.; Mizutani, R.; Nasu, H.; Kamiya, K. *J. Ceram. Soc. Jpn.* **1992**, *100*, 599.
(31) Kozuka, H.; Sakka, S. *Chem. Mater.* **1993**, *5*, 222.
(32) Balzani, V.; Carassitti, V. *Photochemistry of Coordination Compounds;* Academic Press: Glasgow, 1970; p 273.
(33) Weaver, S.; Taylor, D.; Gale, W.; Mills, G. *Langmuir* **1996**, *12*, 4618.
(34) Akbarian, F.; Dunn, B. S.; Zink, J. I. *J. Phys. Chem.* **1995**, *99*, 3892.
(35) Akbarian, F.; Dunn, B. S.; Zink, J. I. *J. Raman Spectrosc.* **1996**, *27*, 775.
(36) Nagahara, L. A.; Tokumoto, H. *Thin Solid Films* **1996**, *281−282*, 647.

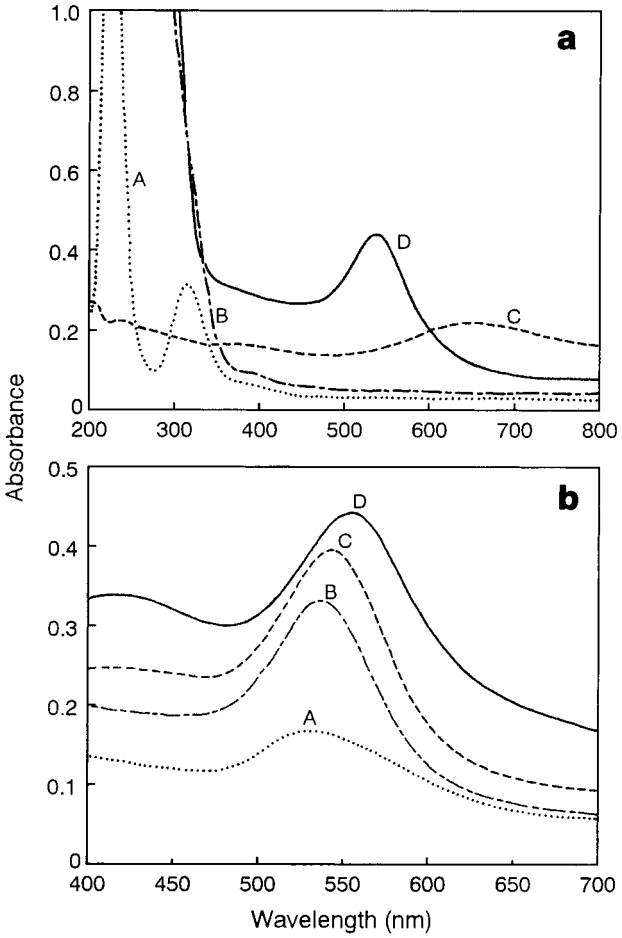

Figure 1. (a) Changes in UV−vis absorption spectra upon photochemical reactions: A, as-deposited Au−SiO_2 film; B, as-deposited Au−SiO_2/TiO_2 film; C, UV-illuminated Au−SiO_2 film; D, UV-illuminated Au−SiO_2/TiO_2 film. The Si:Ti ratio is 1:0 for A and C and is 2:1 for B and D. (b) Visible absorption spectra of Au−SiO_2/TiO_2 films heat-treated at 300 °C for 80 min. The ratio of Si:Ti is 1:0 for A, 4:1 for B, 2:1 for C, and 1:1 for D.

infinity-corrected objective lens and then sent to a photomultiplier via a series of mirrors.

Results and Discussion

Dip-coated Au-doped SiO_2/TiO_2 glassy films having good optical transparency and sufficient mechanical strength were made when the ratio of Si:Ti in the SiO_2/TiO_2 mixture was between 1:0 and 1:1. The dried films were almost colorless but had a faint yellow color due to a UV absorption tail of $AuCl_4^-$ complex ions. Au−SiO_2 films, which contain no TiO_2 (i.e., SiO_2:TiO_2 = 1:0), coated on quartz substrates exhibit the ligand-to-metal charge transfer (LMCT) band of the $AuCl_4^-$ ions[28] centered at 314 nm, as shown by curve A in Figure 1a. In an Au−SiO_2/TiO_2 mixture film, on the other hand, this LMCT band is hidden behind the intense band edge of TiO_2, as shown by curve B in Figure 1a.

When these Au(III)-doped films are illuminated with UV light at ambient conditions, an evolution of color corresponding to surface plasmon bands of metallic Au occurs.[37] The Au−SiO_2/TiO_2 film is deeply stained with violet color due to an absorption band at 500−600 nm as shown by curve D in Figure 1a, whereas the Au−SiO_2 film has a red-shifted weak broad band as shown by curve C in Figure 1a. TEM observations of the films confirm that these absorptions in the visible region correspond to Au particles; electron micrographs of the films are presented in Figure 2a,b. The Au generated in the Au−SiO_2/TiO_2 film forms spherical particles 5−20 nm in diameter, showing their (111) planes with a spacing of 0.235 nm of the face-centered-cubic structure. Note that twinning also occurs (Figure 2a, bottom). The Au−SiO_2 film, in contrast, consists of large, triangular plate-like and needle-like particles which are joined to each other forming networks (Figure 2b). Such networks of particles are known to exhibit broad red-shifted absorption bands.[38] As shown in Figure 3a, the time evolution of the surface plasmon bands indicates that the kinetics for photogeneration of Au particles depends on the ratio of SiO_2/TiO_2 in the matrix films. The absorbances of the Au−SiO_2 film continuously increases to reach a low saturated value. By contrast, curves for the Au−SiO_2/TiO_2 films having lower Ti contents show a certain induction period. After an induction period, the particle formation in the Au−SiO_2/TiO_2 films takes place at a faster reaction rate that is almost the same irrespective of the SiO_2/TiO_2 ratio.

As shown in Figure 1b, the formation of Au particles is also induced by thermal reaction in the dark. This thermal formation is accelerated with an elevation of temperature as well as with increasing Ti content in the SiO_2/TiO_2 mixture films. The absorption bands of Au−SiO_2/TiO_2 films (Figure 1b, B−D) are stronger than that of the Au−SiO_2 film (Figure 1b, A). Since the dip-coated thickness (typically 200 nm here) and the concentration of doped Au(III) ions are nearly the same at all SiO_2/TiO_2 ratios, these different responses suggest that the thermal formation of Au particles is related to the gelation process, especially of the Ti component. The evolution of surface plasmon bands shown in Figure 3b suggests that the thermal generation of Au particles follows the first-order rate law and the rate constant becomes larger with increasing Ti content. It is also noteworthy that the red shifts of the surface plasmon bands of thermally generated Au particles depend on the Ti content (Figure 1b). The maximum absorption wavelengths (λ_{max}) for thermally generated Au particles are plotted in Figure 4 as a function of the Ti/Si ratio. The absorption bands red-shift with increasing Ti content, and these shifts are enhanced by heat treatment at higher temperatures. For photogenerated Au particles, on the other hand, there is no relation between λ_{max} and the Ti/Si ratio.

Comparison of the TEM photographs in Figure 2c,d reveals a clear morphological difference between the Au particles thermally generated in the Au−SiO_2/TiO_2 and Au−SiO_2 films. Those in the latter film are 5−30 nm in diameter and show spherical and truncated triangular morphologies, whereas those in the former films are much larger particles with diameters of 100−200 nm. It thus seems that the observed red shift of the surface plasmon bands (Figure 4) is due to an increase in particle size and an agglomeration effect[22,23] caused by

(37) Halperin, W. P. *Rev. Mod. Phys.* **1986**, *58*, 533 and references therein.

(38) Kreibig, U. Z. *Phys. D.* **1986**, *3*, 239.

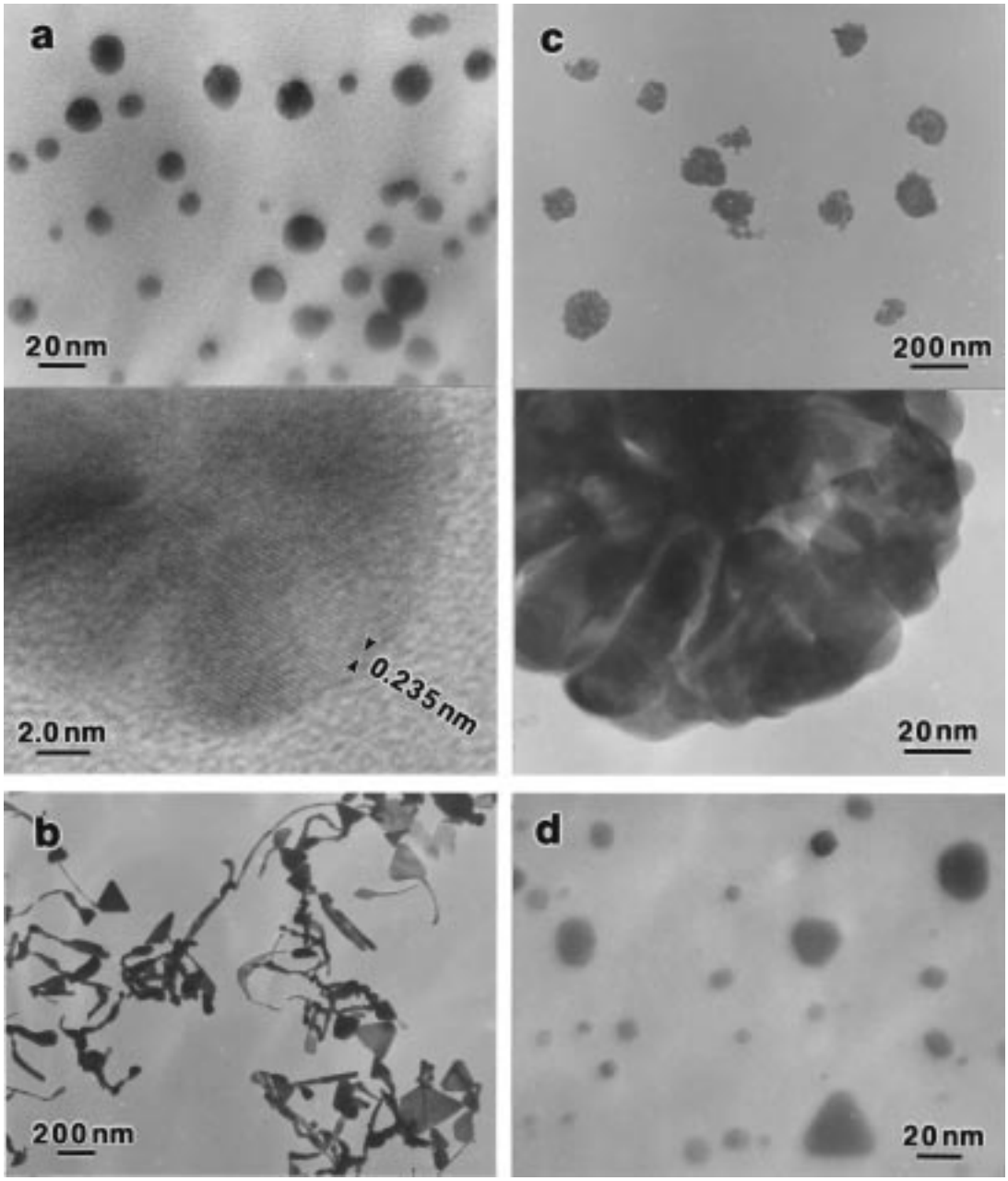

Figure 2. Electron micrographs of photochemically and thermally generated Au particles in $Au-SiO_2$ and $Au-SiO_2/TiO_2$ films. (a) Top: photogenerated Au particles in the $Au-SiO_2/TiO_2$ (Si:Ti = 2:1) film after UV irradiation at room temperature. Bottom: enlarged image showing the (111) plane of a face-centered-cubic Au crystallite. (b) Photogenerated Au particles in the $Au-SiO_2$ film after UV irradiation at room temperature. (c) Top: thermally generated Au particles in the $Au-SiO_2/TiO_2$ (Si:Ti = 2:1) film after heat treatment at 150 °C. Bottom: enlarged image showing that small Au crystallites agglomerate to form large particles. (d) Thermally generated Au particles in the $Au-SiO_2$ film after heat treatment at 300 °C.

higher temperatures as well as to an increase of dielectric constant of matrix films with higher Ti contents.[5,29]

This difference in growth morphology suggests that the Ti component plays an important role in the formation of Au particles. A study of the spontaneous generation of Au particles in a basic methanol solution[28] has indicated that alcohol and hydroxyl ions are required to reduce Au(III) ions to Au(I) ions, in which the alcohol molecules coordinating to the Au(III) ions act as electron donors and the hydroxyl ions neutralize protons formed in the reduction process. This reaction mechanism is unlikely for the present system, however, in which the sol−gel reactions were performed under acidic conditions. In order to examine an effect of the sol−gel process on the particle formation, the matrix films were characterized by IR spectroscopy. Figure 5 shows IR spectra obtained from SiO_2 and SiO_2/TiO_2 (Si:Ti = 2:1) films which were dip-coated and heat-treated at 150 °C (for 5 min) and 450 °C (for 3 h). Because the rate of hydrolysis is much greater for $Ti(OC_2H_5)_4$ than for $Si(OC_2H_5)_4$, the SiO_2/TiO_2 film indicates intense absorption bands of O−H stretching at around 3400 cm^{-1} and Ti−OH stretching at 940 cm^{-1} even after a short heat treatment at 150 °C (Figure 5b, A). In acidic conditions the hydrolysis of starting alkoxides is induced by electrophilic attack of H_3O^+ ions on oxygen atoms of the alkoxyl groups.[39,40] In the thermal formation process this hydrolysis occurs immediately, especially at higher $Ti(OC_2H_5)_4$ contents, and yields the monohy-

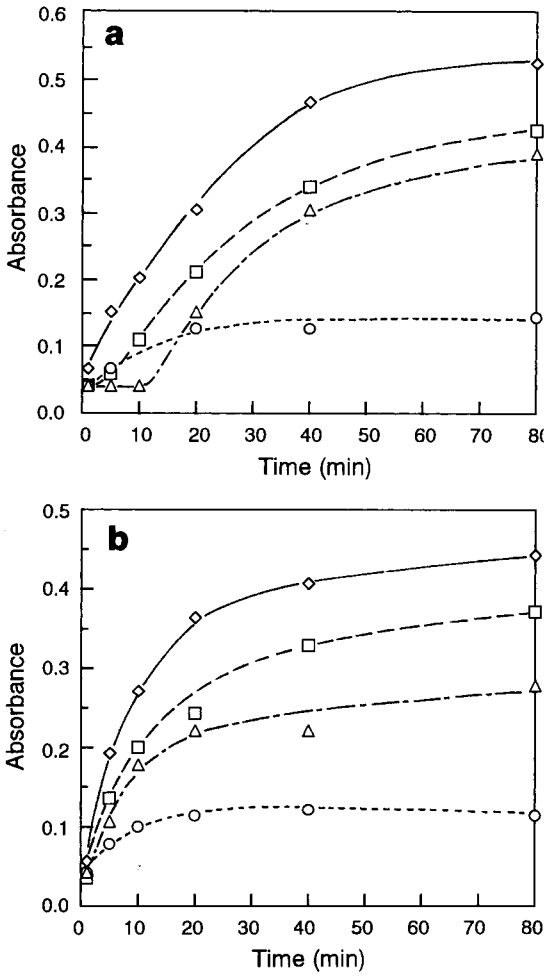

Figure 3. Changes in absorbance at the absorption maxima (λ_{max}) of Au−SiO_2/TiO_2 films with time of photochemical reactions at room temperature (a) and thermal reactions at 300 °C (b). The symbols indicate the Si:Ti ratios in the SiO_2/TiO_2 mixtures: 1:0 (○); 4:1 (△); 2:1 (□); 1:1 (◇).

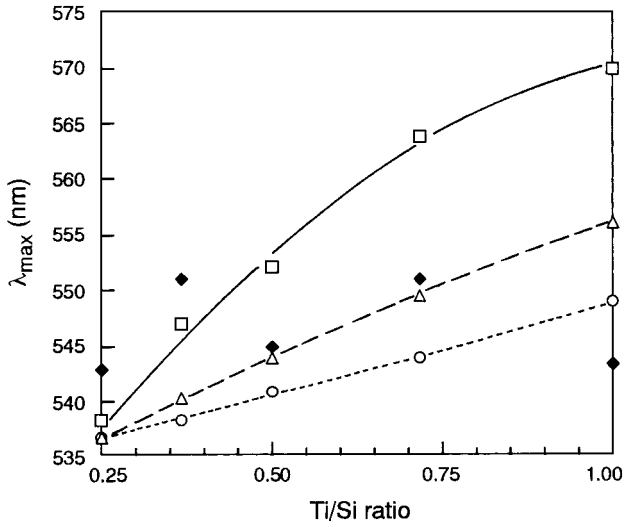

Figure 4. Absorption maximum (λ_{max}) of surface plasmon bands of photochemically and thermally generated Au particles as a function of the Ti/Si ratios in Au−SiO_2/TiO_2 films. (◆) Films UV-illuminated at room temperature for 80 min. The curves are for films thermally treated at (○) 150, (△) 300, and (□) 450 °C.

droxyl species $Ti(OC_2H_5)_3(OH)$. Thus produced hydroxyl groups are probably involved in the reduction of Au-

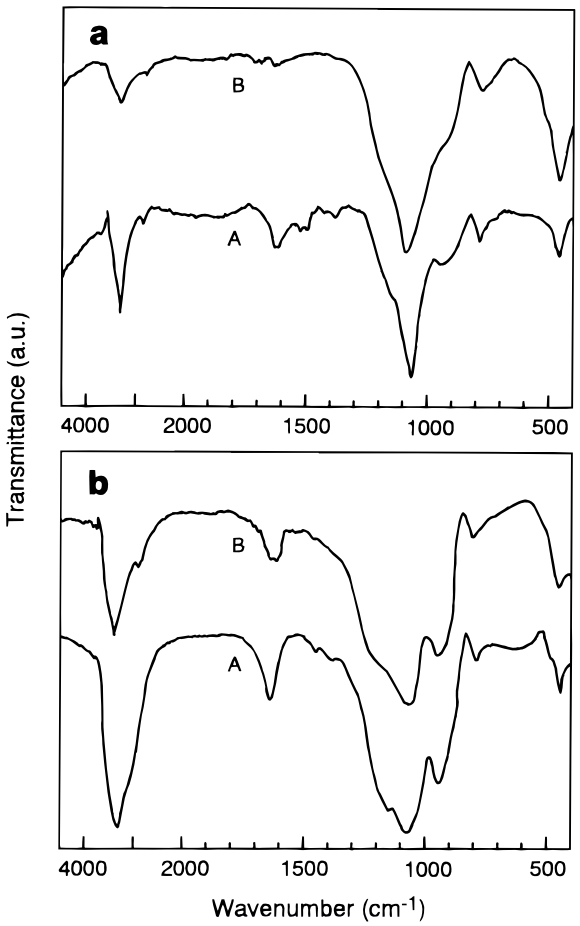

Figure 5. Infrared spectra of SiO_2 (a) and SiO_2/TiO_2 (Si:Ti = 2:1) (b) films: A, heat-treated at 150 °C for 5 min; B, heat-treated at 450 °C for 3 h.

(III) ions. Furthermore, these IR bands of hydroxyl groups considerably remain after a sufficient gelation reaction at 450 °C (Figure 5b, B). It suggests that when water is limited, subsequent hydrolysis of $Ti(OC_2H_5)_3$-(OH) is inhibited, and the condensation of incompletely hydrolyzed species yields a smaller amount of cross-linked polymeric matrixes.[40] Such a loose matrix structure would also enable the doped Au(III) ions to diffuse easily and form large agglomerated metallic particles like those shown in Figure 2c. For the SiO_2 film, in contrast, the IR bands assigned to hydroxyl groups are weaker than those for the SiO_2/TiO_2 film due to a slow hydrolysis reaction of $Si(OC_2H_5)_4$ (Figure 5a, A). After the gelation reaction at 450 °C, the O−H stretching at around 3400 cm^{-1} weakened and the Si−OH stretching at 940 cm^{-1} became a shoulder (Figure 5a, B). It suggests that the gelation by dehydration condensation in the SiO_2 film would produce a densely cross-linked matrix structure that would restrict particle growth. In the photogeneration process of Au particles carried out at room temperature, on the other hand, the hydrolysis reactions occur slowly even in the SiO_2/TiO_2 film. The time evolution curve in Figure 3 (a) indicates that this slow hydrolysis causes the forma-

(39) Aelion, R.; Loebel, A.; Eirich, F. *J. Am. Chem. Soc.* **1950**, *72*, 5705.

(40) Keefer, K. D. *Better Ceramics through Chemistry;* Brinker, C. J., Clark, D. E., Ulrich, D. R., Eds.; North Holland: New York, 1984; p 15.

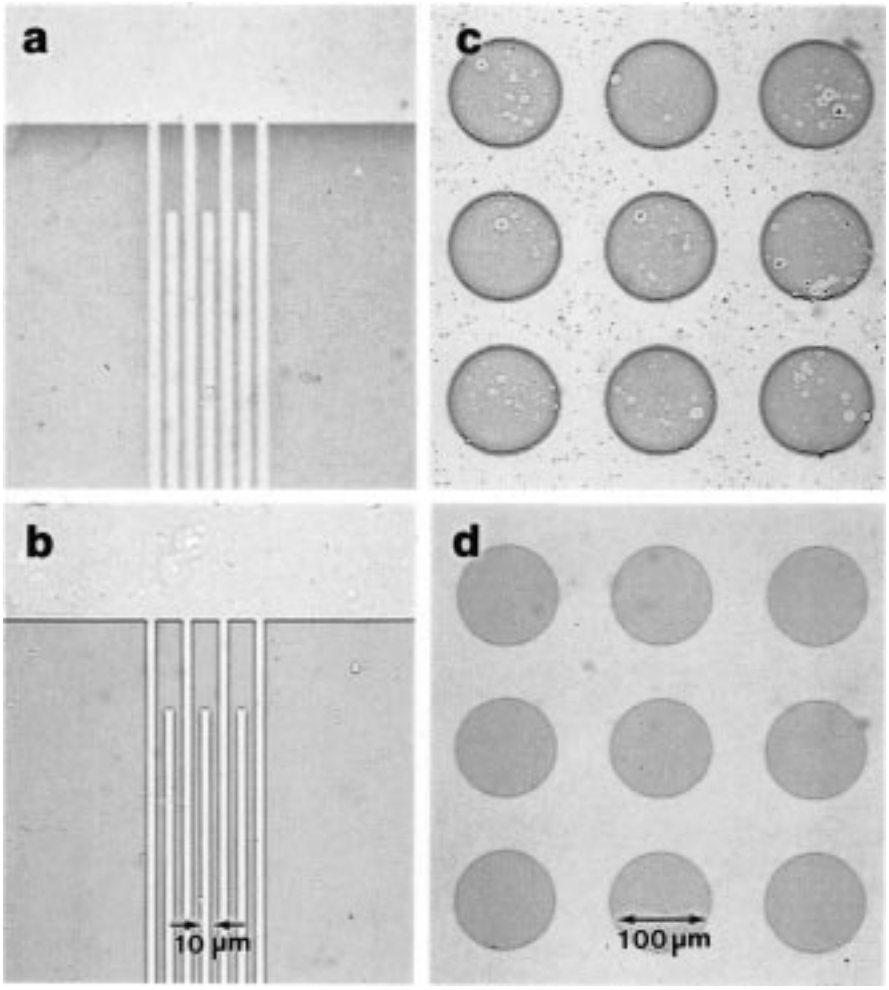

Figure 6. Photomicrographs of $Au-SiO_2/TiO_2$ films photopatterned with Au particles. Comb-like micropatterns of (a) $Au-SiO_2$ and (b) $Au-SiO_2/TiO_2$ (Si:Ti = 2:1) films UV-illuminated at room temperature for 80 min. Disk-like mesh patterns of $Au-SiO_2/TiO_2$ (Si:Ti = 2:1) films UV-illuminated at (c) 5 and (d) 50 °C.

tion of Au particles by photogeneration to be slower than that by thermal generation. Thus, the $Au-SiO_2/TiO_2$ films having low Ti/Si ratios have an induction period.

The photoresponsive formation enables us to use photomasking, beam scanning, etc. to form Au particles in any micropattern in the glassy films. Figure 6a,b shows optical micrographs of photopatterned films of $Au-SiO_2$ and $Au-SiO_2/TiO_2$ that had been exposed to UV light through a comb-like photomask at room temperature. The photopattern in the $Au-SiO_2$ film is not clear due to its lower photoreactivity. The $Au-SiO_2/TiO_2$ film, in contrast, is distinctly photopatterned and shows a consistent gap distance of 10 μm. This photogeneration of Au particles occurs under the synergetic effect of photoinduced and thermal reactions, as seen in the temperature dependence of disk-like photopatterns of Au particles shown in Figures 6c,d. When the $Au-SiO_2/TiO_2$ film is cooled to 5 °C during UV irradiation, photogenerated Au particles form an inhomogeneous pattern with unstained holes in the illuminated disk-like area, and several dark spots are present even in the nonilluminated area. Noteworthily, the contour of the disk pattern is more deeply stained with Au particles than is its inner part. In the film simultaneously heated at 50 °C during UV irradiation, on the other hand, the photogenerated Au particles form a homogeneously stained pattern. This temperature dependence of photogeneration suggests that the generation of Au particles is controlled by the diffusion of Au(III) ions which is dependent on the gelation processes and structures of the matrix films, as mentioned above. The homogeneous evolution of Au particles photopatterned in the Ti-rich matrix films (Figure 6b) can be attributed to the higher mobility of Au ions which is promoted by their loosely polymerized matrix structure, whereas the immobility of Au(III) ions in the cross-linked SiO_2 matrix restrains the particle growth (Figure 6a). To further the photogeneration of Au particles, Au ions are supplied not only within an illuminated area but also from nonilluminated one. In such a matrix film with higher Ti contents, Au ions easily diffuse inside the illuminated area at the moderate temperature of 50 °C (Figure 6d) and are then photoreduced to Au particles. At the low temperature of 5 °C where the ion difusion is limited, Au ions supplied from the nonilluminated outside are photoreduced at the contour of the illuminated area before diffusing inside, and an insufficient supply of Au ions inside the illuminated area results in an inhomogeneous pattern with unstained holes (Figure 6c).

Particle formation in the photoresponsive process was further investigated by NSOM. Figure 7 shows simultaneous topographic and optical images of the $Au-SiO_2/TiO_2$ film photopatterned with a comb-like mask. The

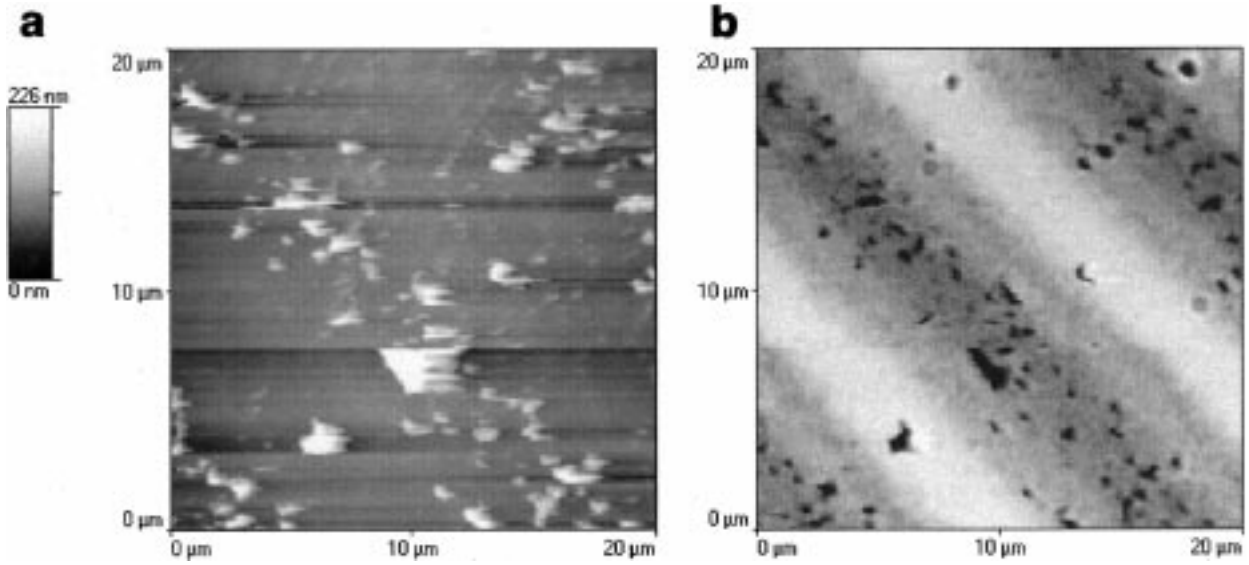

Figure 7. NSOM images of Au−SiO_2/TiO_2 film photopatterned with a comb-like photomask. (a) Topographic image taken by shear-force feedback. (b) Optical transmission image with an Ar-ion-laser probe.

topography in Figure 7a indicates that the film surface is not smooth but is rugged with photogenerated Au particles in the illuminated area. The optical image in Figure 7b indicates that the region illuminated through the comb-like mask has a higher optical density due to absorption at a tail of surface plasmon bands of photogenerated Au particles. Noteworthily, in the photogenerated pattern there are dark spots that almost correspond to the distribution of the rugged topography evident in Figure 7a. These dark spots are probably imaged by scattering of the near-field probe light at large particles sticking out of the film surface. Comparison of the images suggests that smaller particles that are not resolved but give an average contrast in the present NSOM observation are embedded in the matrix film.

To conclude, the present SiO_2/TiO_2 sol−gel system provides an interesting environment in which the generation of Au particles can be controllable by the photochemical/thermal reactions and the SiO_2/TiO_2 ratio. Further investigation of the role of the gelation process in matrix films and of the manipulated formation of particles will enable the production of metal-doped glassy films with properties suitable for device applications.

Acknowledgment. The authors thank T. Tobitani and T. Hishiki (Kobe University) for their help in the sol−gel experiments and thank Mitsuboshi Belting Co. Ltd. for helping us in the microscopic experiments and thickness measurements. H.Y. thanks the Joint Research Center for Atom Technology-National Institute for Advanced Interdisciplinary Research for their support through Researcher Exchange Program. This work was part of a project performed under the Photonics Materials Program by the Venture Business Laboratory of Kobe University.

CM970680D